Mitochondrial Oxidative DNA Damage in Experimental Autoimmune Uveitis

Rahul N. Khurana, Jignesh G. Parikh, Sindhu Saraswathy, Guey-Shuang Wu, and Narsing A. Rao

Purpose. In experimental autoimmune uveitis (EAU), recent work has demonstrated that retinal damage involves oxidative stress early in uveitis, before macrophage cellular infiltration. The purpose of this study was to determine whether oxidative mitochondrial DNA damage occurs early in EAU, before leukocyte infiltration.

Methods. Lewis rats were immunized with S-antigen mixed with complete Freund adjuvant (CFA) to induce EAU. Nonimmunized animals and animals injected with CFA served as controls. Animals were killed on days 3, 4, 7, and 12 after immunization. Damage to mitochondrial DNA and nuclear DNA was assessed using a novel long quantitative polymerase chain reaction technique. TUNEL staining to detect apoptosis and immunohistochemical detection of leukocyte infiltration in EAU retinas were also performed at these times.

Results. Mitochondrial DNA damage occurred early in EAU, from day 4 to day 12. In the early phase of EAU (days 4–7), there was no inflammatory cell infiltration. On day 12 inflammatory cells infiltrated the retina and uvea. Nuclear DNA damage occurred later in EAU at day 12. Neither mitochondrial nor nuclear DNA damage was detected in the controls. TUNEL-positive staining for apoptosis was detected only at day 12 in EAU retina.

Conclusions. Oxidative mitochondrial DNA damage begins at day 4 in EAU, supporting the view that oxidative stress selectively occurs in the mitochondria in the early phase of EAU, before leukocyte infiltration. Such oxidative damage in the mitochondria may be the initial event leading to retinal degeneration in EAU. (*Invest Ophthalmol Vis Sci.* 2008;49: 3299–3304) DOI:10.1167/iovs.07-1607

Intraocular inflammation, commonly referred to as uveitis, is a leading cause of blindness from retinal photoreceptor degeneration. An animal model that closely resembles human uveitis is retinal antigen–induced experimental autoimmune uveitis (EAU).[1] The traditional thinking has attributed the retinal damage in EAU to blood-borne activated macrophages, which are known to generate various toxic agents, including inducible nitric oxide synthase (iNOS), superoxide, and other oxygen-derived reactive agents.[2–5] Macrophages typically infiltrate the retina in the late phase of EAU (days 11–12 after immunization).[6,7] However, in the early phase of EAU (day 5 after immunization), before macrophages and neutrophils infiltrate the retina, recent studies have shown peroxynitrite-mediated nitration of photoreceptor mitochondrial proteins.[8] Reactive oxidants and peroxynitrite are also present in the photoreceptor inner segment mitochondria.[9] Thus, there appears to be oxidative stress in the photoreceptor mitochondria during the early phase of EAU, before the infiltration of the inflammatory cells.

Mitochondrial DNA (mtDNA) is more vulnerable to oxidative damage than nuclear DNA (nDNA) for several reasons.[10,11] mtDNA is in direct contact with the reactive oxygen species (ROS) produced in the mitochondria, and it is not covered by histones or other DNA-associated proteins, thus directly exposing it to ROS.[12] It is an intron-less DNA with a high transcription rate, providing a high probability of oxidative modification of the coding region.[13] Finally, although mitochondria have DNA repair machinery, the repair systems appears to be less efficient.[14,15] Many studies have supported the notion that mtDNA is more susceptible than nDNA to damage by ROS.[10,16–18] Thus, the study of mtDNA offers a reliable biomarker of oxidative stress in tissue rich in mitochondria, such as the retina.

The goal of the present study was to determine whether DNA damage occurs early in EAU. Using a novel long quantitative polymerase chain reaction (QPCR) technique, we showed that mitochondrial oxidative DNA damage occurs early in the EAU (day 4) retina, whereas nDNA damage occurs later (day 12), suggesting the retinal damage may commence early from photoreceptor mitochondrial oxidative stress rather than from macrophage-derived noxious agents.

Methods

Induction of Experimental Uveitis

Lewis rats (virus antibody free; 150–175 g) were obtained from Charles River Laboratory (Wilmington, MA) and were used in all studies. EAU was induced by a hind footpad injection of 60 μg bovine S-antigen in complete Freund adjuvant (CFA) containing 4 mg/mL heat-killed *Mycobacterium tuberculosis* H37 RA (Difco Laboratory, Detroit, MI). Isolation of S-antigen from bovine retina has been described.[19] The antigen was precipitated from bovine retinal extract by half-saturated ammonium sulfate. It was then purified by gel filtration with a hydroxyapatite sorbet (Ultrogel ACA 34; Ciphergen, Fremont, CA), followed by hydroxyapatite chromatography (HA-Ultrogel; Ciphergen). The S-antigen eluates were tested by immunodouble diffusion. At the desired intervals after immunization, animals were euthanatized, and the globes were enucleated. Experiments were conducted immediately after the removal of the retinas. All procedures conformed to the ARVO Statement for the Use of Animals in Ophthalmic and Vision Research.

EAU was induced in 36 Lewis rats; six animals each were killed on postimmunization days 0, 3, 4, 7, 10, and 12, with day 0 corresponding to the nonimmunized control. Six Lewis rats were also immunized with only CFA and were killed at day 12. Three rat retinas were combined as one determination for DNA isolation. All experiments were performed in triplicate for QPCR.

From the Doheny Eye Institute, University of Southern California Keck School of Medicine, Los Angeles, California.

Supported by National Eye Institute Grants EY015714 and EY03040. RNK is a Fight for Sight Postdoctoral Fellow and is supported by Fight for Sight.

Submitted for publication December 14, 2007; revised February 22 and March 27, 2008; accepted June 19, 2008.

Disclosure: **R.N. Khurana**, None; **J.G. Parikh**, None; **S. Saraswathy**, None; **G.-S. Wu**, None; **N.A. Rao**, None

The publication costs of this article were defrayed in part by page charge payment. This article must therefore be marked "*advertisement*" in accordance with 18 U.S.C. §1734 solely to indicate this fact.

Corresponding author: Narsing A. Rao, Doheny Eye Institute, University of Southern California Keck School of Medicine, DVRC 211, 1450 San Pablo Street, Los Angeles, CA 90033; nrao@usc.edu.

In another group of 24 Lewis rats, EAU was induced with the use of bovine S-antigen. Three animals each were killed on postimmunization days 3, 4, 7, and 12, with day 0 corresponding to the nonimmunized control. Six other Lewis rats were immunized with only CFA and killed on day 12. The globes were enucleated, and the retinas were used for (TdT)–mediated dUTP-biotin nick end labeling (TUNEL) staining for apoptosis detection and for CD68, CD45, and CD11b immunostaining.

A positive control for oxidative DNA damage involving the exposure of rat retina explants to 3-morpholinosydnonimine (SIN-1) for 6 hours in vitro was also performed.[8]

DNA Isolation and QPCR

Total cellular DNA was isolated with a DNA kit (Easy-DNA Kit; Invitrogen, Carlsbad, CA), according to the manufacturer's protocol. DNA isolation by this technique results in genomic preparation suitable for long QPCR. Total cellular DNA concentration was determined with dye (PicoGreen dye in the Quanti-iT High Sensitivity DNA Assay Kit; Invitrogen, Carlsbad, CA), and fluorescence was measured with a fluorometer (Qubit; Invitrogen). The dye (PicoGreen in the Quanti-iT High Sensitivity DNA Assay Kit; Invitrogen) is essentially nonfluorescent and exhibits more than 1000-fold fluorescence enhancement on binding to dsDNA at an excitation wavelength of 480 nm and an emission wavelength of 530 nm. The assay, with a linear detection range of 0.2 to 1000 ng, is extremely sensitive for dsDNA.

QPCR was performed (via the GeneAmp PCR system 9700 with the GeneAmp XL PCR kit; Applied Biosystems, Foster City, CA) according to a protocol described previously except that the QPCR products were made with the assay kit (Quanti-IT High Sensitivity DNA Assay Kit; Invitrogen).[10,20] Reaction mixtures contained 15 ng genomic DNA template; reagent conditions for the QPCR have been described previously.[20] Primer sequences used were as follows: for the 12.5-kb nuclear gene, clusterin 5′-AGA CGG GTG AGA CAG CTG CAC CTT TTC-3′ and 5′-CGA GAG CAT CAA GTG CAG GCA TTA GAG-3′; for the 13.4-kb mitochondrial genome, 5′-AAA ATC CCC GCA AAC AAT GAC CAC CC-3′ and 5′-GGC AAT TAA GAG TGG GAT GGA GCC AA-3′. As previously described, sample quality was also tested by QPCR of a 235-bp mitochondrial fragment (5′-CCT CCC ATT CAT TAT CGC CGC CCT TGC-3′ and 5′-GTC TGG GTC TCC TAG TAG GTC TGG GAA-3′) with the expectation that equal template concentrations should yield similar QPCR (short) concentrations.

DNA lesion frequencies were calculated as described previously.[10] Briefly, the amplification of damaged samples (A_D) was normalized to the amplification of undamaged control (A_0), resulting in a relative amplification ratio. The undamaged control (A_0) involved the nonimmunized control. Assuming a random distribution of lesions and using the Poisson equation [$f(x) = e^{-\lambda}\lambda^x/x!$, where λ = the average lesion frequency] for the undamaged template (i.e., the zero class; $x = 0$), the average lesion frequency per DNA stand was determined as $\lambda = -\ln A_D/A_0$.[10] Statistical analysis was performed with a Student's *t*-test, with $P < 0.05$ considered significant.

Apoptosis Detection

All globes were fixed with formalin and embedded in paraffin. A TUNEL staining kit (R&D Systems, Minneapolis, MN) was used to detect apoptosis, as described by the manufacturer. Briefly, paraffin sections were deparaffinized and treated with proteinase K for 15 minutes and were washed. Endogenous peroxidase was quenched by incubation with 3% H_2O_2 for 5 minutes. The sections were then incubated with the TdT for 1 hour at 37°C. Streptavidin-fluorescein conjugate was applied to the sections. After they were washed in phosphate-buffered saline (PBS)/Tween-20, sections were mounted with medium with 4′6-diamidino-2-phenylindole (Vector Laboratories, Burlingame, CA). Subsequently, sections were visualized under a confocal microscope (Carl Zeiss, Thornwood, NY). PBS was used in place of TdT enzyme as the negative control, and known positive slides with apoptotic cells were used as positive controls.

Immunohistochemical Staining for Leukocytes, Macrophages, and Microglia

Cryostat sections of retina (10 μm) were incubated with mouse anti–rat CD45 (1:100; BD Biosciences, San Jose, CA) overnight at 4°C. The slides were then incubated with the secondary antibody, biotin-labeled mouse anti–rat IgG (Dako, Carpinteria, CA). After enhancement with a complex of peroxidase-conjugated biotin and avidin (ABC Kit; Vector Laboratories), visualization was carried out with the use of 3-diamino-9-ethylcarbazole.

To detect macrophages with the CD68 marker, paraffin sections from control, day 7, and day 12 postimmunization retina were deparaffinized and subjected to antigen retrieval by covering the sections with 10 M sodium citrate buffer (pH 6.0), and heating them for 15 seconds. Slides were then cooled to room temperature for 20 minutes, rinsed with PBS, and blocked with 2% bovine serum albumin for 30 minutes at room temperature. Sections were incubated overnight at 4°C with mouse monoclonal anti–rat CD68 antibody (1:100; BD Biosciences, San Jose, CA). Sections were washed three times with PBS/0.05% Tween-20 and then incubated in the dark for 1 hour at room temperature with horse anti–mouse IgG conjugated with fluorescein (1:100; Vector Laboratories). The sections were then washed with PBS/Tween-20 and mounted with medium containing 4′,6-diamidino-2-phenylindole (Vector Laboratories) and were viewed under a confocal microscope (Carl Zeiss). Isotype control and primary antibody replaced by PBS were used as negative controls. The sections of spleen were used as positive controls.

For detecting retinal microglia, cryosections (10 μm) were incubated with mouse anti–rat CD11b (1:200; Serotec, Oxford, UK), and fluorescein-conjugated horse anti–mouse IgG (Vector) was used as secondary antibody. Isotype control and primary antibody replaced by PBS were used as control procedures to ascertain the specificity of the primary antibody. Sections were visualized with a laser scanning confocal microscope (LSM-510; Carl Zeiss).

Results

EAU and DNA Damage

To investigate whether oxidative DNA damage occurs in early EAU, a well-validated and sensitive QPCR assay was used. The approach is based on the premise that DNA lesions, including oxidative damage that cause strand breaks, base modification, and abasic sites,[21] will block the progression of the polymerase, resulting in decreased amplification of the target sequence.[20] DNA damage was quantified by comparing the relative efficiency of amplification of large fragments of DNA (13.4 kb for the mtDNA and 12.5 kb for the nDNA) and normalizing this to the amplification of smaller (<250 bp) fragments that have a statistically negligible likelihood of containing damaged bases, thus normalizing differences in copy number.[10]

A decrease in mtDNA amplification began early in EAU at day 4 and continued through days 7 and 12 after S-antigen immunization (Fig. 1A). A positive control for oxidative DNA damage involving exposure of the rat retina to SIN-1 for 6 hours in vitro[8] was also performed. SIN-1, which is a peroxynitrite donor, simultaneously releases nitric oxide and superoxide and causes oxidative stress in an in vitro system of retinal photoreceptor cells.[8] The positive control with SIN-1 showed a decrease in mtDNA amplification. On day 12, a CFA control without S-antigen immunization did not show any changes in DNA amplification (Fig. 1A). A decrease in nDNA amplification occurred later that day, after S-antigen immunization (Fig. 1B), but there were no changes in the nonimmunized, CFA-injected control. The SIN-1–positive control did show a decrease in nDNA amplification (Fig. 1B).

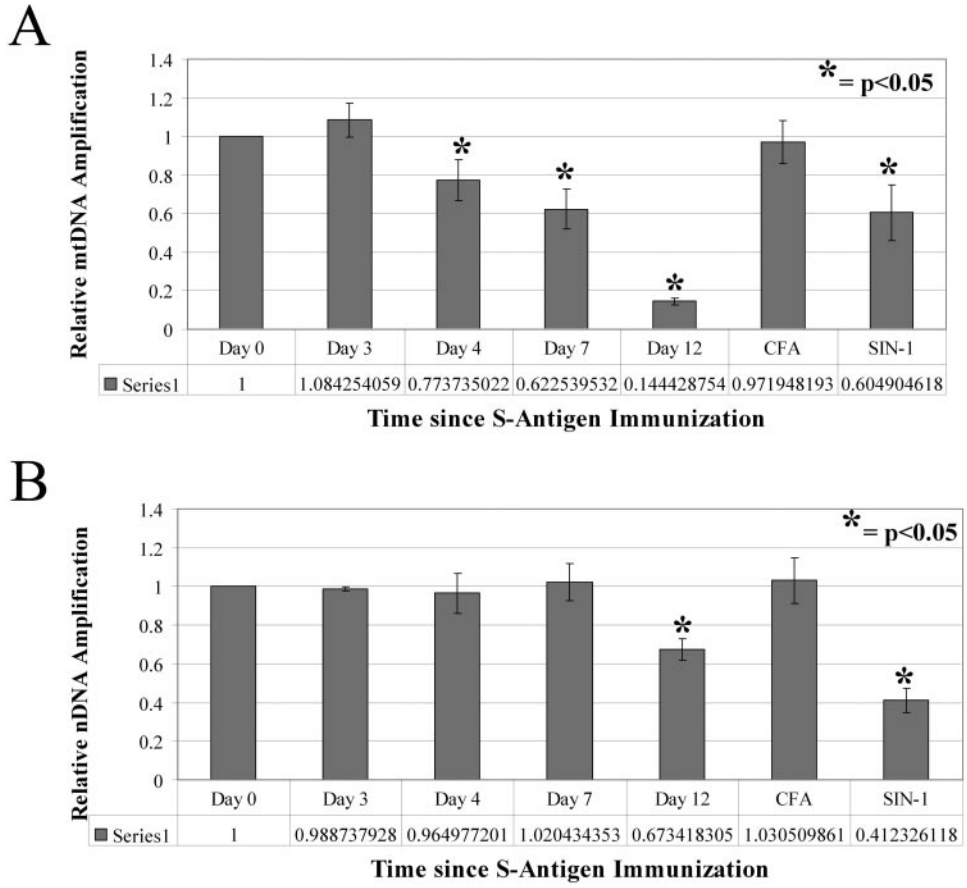

FIGURE 1. Decrease in DNA amplification of the mitochondrial and nuclear genomes in EAU. (**A**) Decrease in mtDNA amplification at day 4 that continues through days 7 and 12 after S-antigen immunization. There was no change in mtDNA amplification with the CFA control, and there was a decrease with the positive in vitro control involving SIN-1. (**B**) There was a decrease in nDNA amplification at day 12 after immunization. There was no change in nDNA amplification with the CFA control, but there was a decrease with the positive in vitro control involving SIN-1. Relative amplification values are given as mean ± SE. All values represent three independent experiments.

DNA lesion frequencies were calculated assuming a random distribution of lesions and using the Poisson equation: $f(x) = e^{-\lambda}\lambda^x/x!$, where λ = the average lesion frequency for the undamaged template.[10] The amplification of damaged samples (A_D) was normalized to the amplification of undamaged control (A_0). The undamaged control (A_0) involved the nonimmunized control. The average lesion per DNA strand was determined as $\lambda = -\ln A_D/A_0$.[10] mtDNA damage occurred early in EAU beginning at day 4 and continuing throughout until day 12, whereas nDNA damage occurred later at day 12 (Fig. 2).

Apoptosis, Leukocytes, Macrophages, and Microglia in EAU

To determine whether apoptosis was occurring in the retinal photoreceptors, a TUNEL staining kit was used to measure DNA fragmentation. TUNEL-positive cells were absent at day 3 (Fig. 3A), day 4 (Fig. 3B), and day 7 (Fig. 3C) and was first seen at day 12 after immunization (Fig. 3D). The TUNEL-positive cells are located in the retinal photoreceptor layer. The nonimmunized controls, CFA-injected animals, and negative controls did not have any TUNEL-positive cells (data not shown).

Detection for inflammatory leukocytes and retinal immune cells, microglia, was carried out on days 7 (early phase) and 12 (amplification phase). At day 7, a small number of $CD45^+$ cells were seen only in the choroid (Fig. 4A), whereas at day 12, positive cells were detected in the choroid and in the nuclear layers and nerve fiber layer (Fig. 4B). At day 12, the disruption of the nuclear layer was also observed (Fig. 4B). No $CD68^+$ cells were seen in day 7 retinas (Fig. 4C), but numerous cells were present in the inner retina and inner nuclear layer at day 12 (Fig. 4D). At day 7 after infection, the resident microglia are seen mostly at the inner nuclear layer (Fig. 4E). At day 12 after

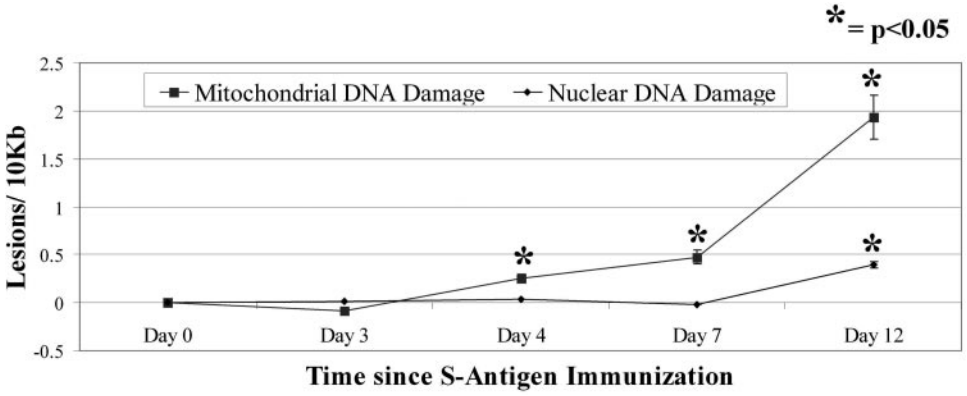

FIGURE 2. DNA damage occurs in EAU. The graph represents the number of DNA lesions per 10 kb as determined by QPCR of mitochondrial and nuclear genomes. Mitochondrial DNA damage begins at day 4 and increases throughout until day 12 in EAU. Nuclear DNA damage occurs later at day 12. All values represent three independent experiments. Vertical bars indicate SE.

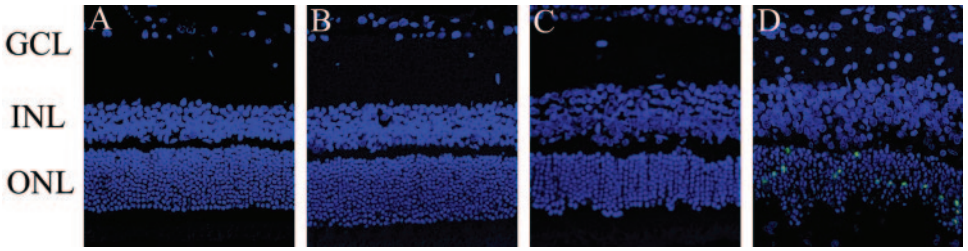

FIGURE 3. Detection of apoptosis and leukocytes in EAU. No TUNEL-positive (apoptotic) photoreceptor cells are detected on day 3 (**A**), day 4 (**B**), or day 7 (**C**) after immunization. TUNEL-positive (apoptotic) photoreceptor cells are seen in the outer nuclear layer in the retina on day 12 after immunization (**D**). GCL, ganglion cell layer; INL, inner nuclear layer; ONL, outer nuclear layer. Original magnification, ×30.

infection, however, most microglia migrated to the photoreceptor layer (Fig. 4F).

DISCUSSION

In this study, using a novel long QPCR technique, we determined that mitochondrial oxidative DNA damage occurs early in EAU (day 4) and increases throughout EAU, whereas nuclear DNA damage occurs later (day 12). Before the development of the long QPCR technique, it was difficult to reliably detect mtDNA damage. Early studies used DNA extraction techniques that caused extensive DNA oxidation and resulted in reports of artifactually high levels of adducts.[22] Furthermore, techniques to isolate mitochondria from whole-cell (tissue) extracts to obtain nDNA-free mtDNA might also have caused higher levels of damage in mtDNA.[23] In EAU, there was evidence of oxidative damage involving lipids and proteins.[6] With the long QPCR technique, mtDNA damage could be detected in EAU. The long QPCR technique is well validated, sensitive, and reliably assay based on the principle that oxidative DNA lesions inhibit DNA polymerases.[10] The current detection limits are one to two lesions per 10^5 nucleotides with 5 to 15 ng mammalian DNA (equivalent to approximately 1000–3000 cells).[13]

However, there are limitations associated with QPCR. First, DNA lesions that do not significantly stall the progression of DNA polymerase, such as 8-hydroxydeoxygenase, are not detected with high efficiency.[20] In this study, this is not pertinent because oxidative stress is unlikely to produce only one type of lesion.[24] Oxidative DNA damage produces a wide variety of DNA lesions, including oxidation of purines or pryimidines, abasic sites, and single-strand breaks.[21] Second, although the presence of damage on the DNA template can be identified, the specific nature of the lesion cannot be determined by QPCR alone.[20]

mtDNA is prone to oxidative damage because it is in direct contact with the ROS produced in the mitochondria and it lacks histones, which make it vulnerable to oxidative damage. Thus, mtDNA is a reliable biomarker of oxidative stress. In this study, mtDNA is damaged early in EAU, beginning at day 4 after immunization. Mitochondrial oxidative stress occurs in EAU before the infiltration of the macrophages on days 11 to 12. This supports previous studies that showed peroxynitrite-mediated nitration of photoreceptor mitochondrial proteins occurs in the mitochondrial photoreceptors at day 5.[8] Furthermore, reactive oxidants and peroxynitrite are present in the photoreceptor inner segment mitochondria at day 5 as well.[9] mtDNA appears to be the first affected by the oxidative stress in EAU. Protein nitration first occurs at day 5,[6] supporting that oxidative stress in the photoreceptor mitochondria occurs during the early phase of EAU, before the migration of macrophages and microglia. The mitochondria also appear to be the original site of inflammatory insult involving oxidative stress in early EAU.

The mechanism that induces oxidative stress in early EAU is unclear. Oxidative damage was originally attributed to the macrophages, but there is no histologic or immunohistochemical evidence of their presence until day 11 to 12.[6,7] Retinal microglia have recently been shown to exhibit phagocytic and pathogenic functions similar to those of macrophages. However, they are only detected until days 9 and 10 after immunization.[7] There is some evidence implicating T cells in the pathogenesis of the early oxidative stress and insult in EAU. A few $CD3^+$ cells were found in the retina on day 5 after immunization, and real-time QPCR showed a 1.98 increase in CD28 transcripts.[9] There is a significant upregulation of TNFα, INOS, IFNγ, and IL1α at day 5 after immunization,[9] and these cytokines are associated with the induction of oxidative stress. The timing of their presence coincides with the mtDNA damage. There is a significant increase in TNFα at day 3 (Saraswathy S, et al., unpublished observation, 2006), which may explain the early mtDNA damage that occurs at day 4. Such early upregulation of TNFα suggests that innate immunity could contribute to oxidative stress during early EAU. TNFα expression is known to upregulate iNOS and the subsequent production of nitric oxide and oxidant species.[25–28] Although mitochondrial DNA damage occurs before leukocyte infiltration in the retina, the mechanism for such damage is unclear. It is plausible that the innate immune response may be the cause of the early oxidative insult before the priming and arrival of the T cells into the retina. Further studies are needed to clarify the role of innate immunity in the initiation of mitochondrial oxidative stress in early EAU.

mtDNA is an important target for oxidative damage and, if not repaired, can lead to mitochondria dysregulation and cell death.[29] mtDNA damage leads to loss of membrane potential, adenosine triphosphate synthesis, and, ultimately, cell death in many in vitro systems.[11,30,31] Interestingly, in our study, apoptosis was not detected until much later, on day 12. The reasons early cell death did not occur may be several. First, the sensitivity of the TUNEL assay might not have been high enough to detect apoptosis because of the mtDNA damage as shown through QPCR. Further studies involving PCR-based gene array screening involving apoptosis and its signaling pathway may reveal that apoptotic changes occur before detection by TUNEL in EAU. Second, the amount of mtDNA damage necessary to set off the apoptotic cascades might not have been sufficient until day 12. Third, protective mechanisms early in EAU might have prevented apoptosis despite the presence of oxidative stress. Oxidative stress is known to upregulate a variety of heat shock proteins and crystallins. These heat shock proteins have antiapoptotic effects by specifically inhibiting components of apoptotic machinery.[32–39] In early EAU, αA crystallin is upregulated and prevents apoptosis by binding to nitrated cytochrome *c*.[40] This may explain why there was no apoptosis early in EAU despite the presence of mtDNA damage. Moreover, oxidative stress could have been overwhelming on

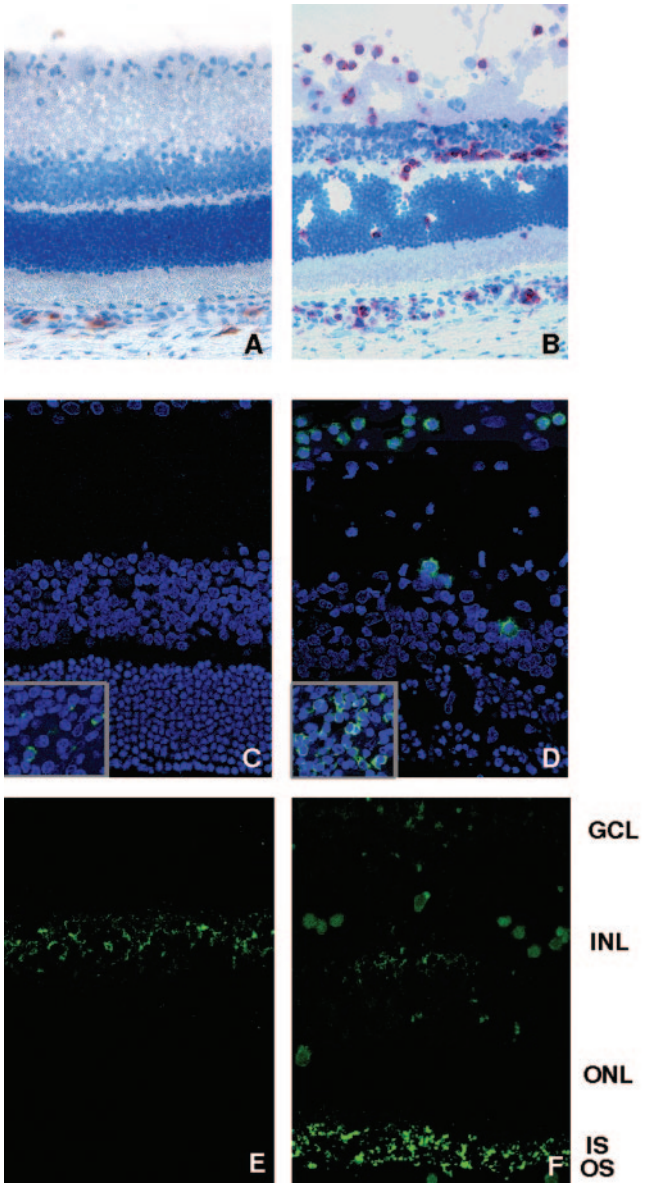

FIGURE 4. (**A**–**F**) Immunolocalization of $CD45^+$, $CD68^+$, and $CD11b^+$ cells in the retina on days 7 and 12 after immunization. A few $CD45^+$ cells were detected in the choroid on day 7, but the retina was negative for such cells (**A**). Large numbers of CD45 cells were seen in the retina and choroid on day 12 (**B**). Similarly, a few $CD68^+$ cells were seen in the choroid on day 7 (**C**, *inset*), whereas the retina was negative for such cells. Numerous $CD68^+$ cells were detected in the choroid (**D**, *inset*) and retina on day 12 (**D**). $CD11b^+$ cells were present predominantly in the inner nuclear layer of day 7 retinas (**E**). A few cells were also detected in the inner plexiform layer. On day 12 after immunization, a large number of $CD11b^+$ cells were localized in the photoreceptor inner and outer segments. They were also present in the inner nuclear layer, outer plexiform layer, and other parts of retina on day 12 (**F**). IS, inner segment; OS, outer segment.

day 12 from the infiltration of activated macrophages, and the defensive antiapoptotic proteins might not have kept up with the enhanced stress.

References

1. Nussenblatt RB. Bench to bedside: new approaches to the immunotherapy of uveitic disease. *Int Rev Immunol*. 2002;21:273–289.
2. Rao NA, Wu GS. Free radical mediated photoreceptor damage in uveitis. *Prog Retin Eye Res*. 2000;19:41–68.
3. Forrester JV, Huitinga I, Lumsden L, Dijkstra CD. Marrow-derived activated macrophages are required during the effector phase of experimental autoimmune uveoretinitis in rats. *Curr Eye Res*. 1998;17:426–437.
4. Jiang HR, Lumsden L, Forrester JV. Macrophages and dendritic cells in IRBP-induced experimental autoimmune uveoretinitis in B10RIII mice. *Invest Ophthalmol Vis Sci*. 1999;40:3177–3185.
5. Wu GS, Zhang J, Rao NA. Peroxynitrite and oxidative damage in experimental autoimmune uveitis. *Invest Ophthalmol Vis Sci*. 1997;38:1333–1339.
6. Wu GS, Lee TD, Moore RE, Rao NA. Photoreceptor mitochondrial tyrosine nitration in experimental uveitis. *Invest Ophthalmol Vis Sci*. 2005;46:2271–2281.
7. Rao NA, Kimoto T, Zamir E, et al. Pathogenic role of retinal microglia in experimental uveoretinitis. *Invest Ophthalmol Vis Sci*. 2003;44:22–31.
8. Ito S, Wu GS, Kimoto T, Hisatomi T, Ishibashi T, Rao NA. Peroxynitrite-induced apoptosis in photoreceptor cells. *Curr Eye Res*. 2004;28:17–24.
9. Rajendram R, Saraswathy S, Rao NA. Photoreceptor mitochondrial oxidative stress in early experimental autoimmune uveoretinitis. *Br J Ophthalmol*. 2007;91:531–537.
10. Yakes FM, Van Houten B. Mitochondrial DNA damage is more extensive and persists longer than nuclear DNA damage in human cells following oxidative stress. *Proc Natl Acad Sci U S A*. 1997;94:514–519.
11. Santos JH, Hunakova L, Chen Y, Bortner C, Van Houten B. Cell sorting experiments link persistent mitochondrial DNA damage with loss of mitochondrial membrane potential and apoptotic cell death. *J Biol Chem*. 2003;278:1728–1734.
12. Ljungman M, Hanawalt PC. Efficient protection against oxidative DNA damage in chromatin. *Mol Carcinog*. 1992;5:264–269.
13. Liang FQ, Godley BF. Oxidative stress-induced mitochondrial DNA damage in human retinal pigment epithelial cells: a possible mechanism for RPE aging and age-related macular degeneration. *Exp Eye Res*. 2003;76:397–403.
14. Croteau DL, Bohr VA. Repair of oxidative damage to nuclear and mitochondrial DNA in mammalian cells. *J Biol Chem*. 1997;272:25409–25412.
15. Mandavilli BS, Santos JH, Van Houten B. Mitochondrial DNA repair and aging. *Mutat Res*. 2002;509:127–151.
16. Salazar JJ, Van Houten B. Preferential mitochondrial DNA injury caused by glucose oxidase as a steady generator of hydrogen peroxide in human fibroblasts. *Mutat Res*. 1997;385:139–149.
17. Ballinger SW, Van Houten B, Jin GF, Conklin CA, Godley BF. Hydrogen peroxide causes significant mitochondrial DNA damage in human RPE cells. *Exp Eye Res*. 1999;68:765–772.
18. Mandavilli BS, Ali SF, Van Houten B. DNA damage in brain mitochondria caused by aging and MPTP treatment. *Brain Res*. 2000;885:45–52.
19. Rao NA. Role of oxygen free radicals in retinal damage associated with experimental uveitis. *Trans Am Ophthalmol Soc*. 1990;88:797–850.
20. Santos JH, Meyer JN, Mandavilli BS, Van Houten B. Quantitative PCR-based measurement of nuclear and mitochondrial DNA damage and repair in mammalian cells. *Methods Mol Biol*. 2006;314:183–199.
21. Demple B, Harrison L. Repair of oxidative damage to DNA: enzymology and biology. *Annu Rev Biochem*. 1994;63:915–948.
22. Helbock HJ, Beckman KB, Shigenaga MK, et al. DNA oxidation matters: the HPLC-electrochemical detection assay of 8-oxo-deoxyguanosine and 8-oxo-guanine. *Proc Natl Acad Sci U S A*. 1998;95:288–293.
23. Anson RM, Hudson E, Bohr VA. Mitochondrial endogenous oxidative damage has been overestimated. *FASEB J*. 2000;14:355–360.
24. Termini J. Hydroperoxide-induced DNA damage and mutations. *Mutat Res*. 2000;450:107–124.
25. Savion S, Oddo S, Grover S, Caspi RR. Uveitogenic T lymphocytes in the rat: pathogenicity vs. lymphokine production, adhesion molecules and surface antigen expression. *J Neuroimmunol*. 1994;55:35–44.

26. Borutaite V, Morkuniene R, Brown GC. Release of cytochrome *c* from heart mitochondria is induced by high Ca^{2+} and peroxynitrite and is responsible for Ca(2+)-induced inhibition of substrate oxidation. *Biochim Biophys Acta*. 1999;1453:41–48.
27. Moreno-Sanchez R. Regulation of oxidative phosphorylation in mitochondria by external free Ca^{2+} concentrations. *J Biol Chem*. 1985;260:4028–4034.
28. Rizzuto R, Pinton P, Carrington W, et al. Close contacts with the endoplasmic reticulum as determinants of mitochondrial Ca^{2+} responses. *Science*. 1998;280:1763–1766.
29. Van Houten B, Woshner V, Santos JH. Role of mitochondrial DNA in toxic responses to oxidative stress. *DNA Repair (Amst)*. 2006; 5:145–152.
30. Deng G, Su JH, Ivins KJ, Van Houten B, Cotman CW. Bcl-2 facilitates recovery from DNA damage after oxidative stress. *Exp Neurol*. 1999;159:309–318.
31. Mandavilli BS, Boldogh I, Van Houten B. 3-Nitropropionic acid-induced hydrogen peroxide, mitochondrial DNA damage, and cell death are attenuated by Bcl-2 overexpression in PC12 cells. *Brain Res Mol Brain Res*. 2005;133:215–223.
32. Beere HM, Wolf BB, Cain K, et al. Heat-shock protein 70 inhibits apoptosis by preventing recruitment of procaspase-9 to the Apaf-1 apoptosome. *Nat Cell Biol*. 2000;2:469–475.
33. Saleh A, Srinivasula SM, Balkir L, Robbins PD, Alnemri ES. Negative regulation of the Apaf-1 apoptosome by Hsp70. *Nat Cell Biol*. 2000;2:476–483.
34. Bruey JM, Ducasse C, Bonniaud P, et al. Hsp27 negatively regulates cell death by interacting with cytochrome *c*. *Nat Cell Biol*. 2000; 2:645–652.
35. Mehlen P, Kretz-Remy C, Preville X, Arrigo AP. Human hsp27, *Drosophila* hsp27 and human αB-crystallin expression-mediated increase in glutathione is essential for the protective activity of these proteins against TNFα-induced cell death. *EMBO J*. 1996;15: 2695–2706.
36. Kamradt MC, Chen F, Cryns VL. The small heat shock protein alpha B-crystallin negatively regulates cytochrome *c*- and caspase-8-dependent activation of caspase-3 by inhibiting its autoproteolytic maturation. *J Biol Chem*. 2001;276:16059–16063.
37. Pandey P, Farber R, Nakazawa A, et al. Hsp27 functions as a negative regulator of cytochrome *c*-dependent activation of procaspase-3. *Oncogene*. 2000;19:1975–1981.
38. Garrido C, Bruey JM, Fromentin A, Hammann A, Arrigo AP, Solary E. HSP27 inhibits cytochrome *c*-dependent activation of procaspase-9. *FASEB J*. 1999;13:2061–2070.
39. Pandey P, Saleh A, Nakazawa A, et al. Negative regulation of cytochrome *c*-mediated oligomerization of Apaf-1 and activation of procaspase-9 by heat shock protein 90. *EMBO J*. 2000;19:4310–4322.
40. Rao NA, Saraswathy S, Wu GS, Katselis GS, Wawrousek EF, Bhat S. Elevated retina-specific expression of the small heat shock protein, αA-crystallin is associated with photoreceptor protection in experimental autoimmune uveitis. *Invest Ophthalmol Vis Sci*. 2008;49: 1161–1171.